This manuscript was accepted by Appl. Phys. Lett. Click here to see the version of record.

The significance of grain morphology, moisture and strain rate on the rapid compaction of silica sands

J. I. Perry[1], C. H. Braithwaite[1], N. E. Taylor[1], A. D. Pullen[2] and A. P. Jardine[1]

[1]*Cavendish Laboratory, JJ Thomson Avenue, Cambridge CB3 0HE, United Kingdom*

[2]*Department of Civil and Environmental Engineering, Imperial College London, SW7 2AZ, United Kingdom*

There is considerable interest in the high-rate compaction of brittle granular materials such as sand. However, the vast majority of studies focus on a single granular system, limiting our ability to make comparisons between materials to discern how granular structure manifests as bulk material response. Here, three different silica sands with similar grain size and shape are studied: we compare a rough quarry sand, a smoother-grained sand, and a sandy loam. Quasi-static compaction and planar shock loading responses are compared, and recovered samples analyzed. The combination provides information regarding the interplay between granular properties, loading conditions and material response. We show that the fundamental grain-scale behaviour depends on loading conditions: At low strain rates compaction behaviour is dominated by grain morphology, and in particular smoothness and particle size distribution. Under shock loading, grain rearrangement and force chain effects are suppressed, and the nature of inter-granular contact points, modified by the presence of moisture or fines, is most important. Furthermore, grain fracture under shock loading is substantially reduced with increasing moisture content.

Electronic mail: jip24@cantab.net

The processes by which brittle granular materials compact largely depend on their microstructure and the properties and interactions of the grains themselves. Predicting the dynamic response of these systems requires knowledge of how grain-scale phenomena manifest as macroscopic response. Such insight is crucial for a wide range of high rate applications including planetary formation and impact cratering[1], the response to blast and penetration[2], and predicting and improving soil response to earthquakes and landslips through seismic coupling[3].

Developing a detailed knowledge of granular systems requires a sustained theoretical[4] and experimental[5] effort. Experimental data is required to guide and populate material models, which otherwise struggle to predict how nonlinear grain-scale phenomena affect macroscopic behaviour. Shock compaction of dry sand has been the focus of a number of studies[6-9], with a few probing the additional effects of moisture[10-12]. The authors have previously detailed the shock-release cycle in dry[13] and wetted[14] sand.

While experimental efforts to date have provided substantial information on the compaction of sands, each study almost invariably probes a single granular material. In addition, there is often substantial variation

in sample preparation and experimental techniques between studies. There is, therefore, a lack of understanding of the effects of changing morphology, moisture and strain rate[5], although it is known that the dynamic response depends strongly on factors such as grain shape, size, porosity, surface roughness and arrangement[15]. Predictive modelling capability therefore remains limited[16, 17]. While studies directly comparing the rapid response of different sands are lacking, a number of studies highlight how further research is needed. Studies on glass spheres have shown that for stresses below that required for full compaction, systems of smaller particles densify less than larger ones[18], while the particle size distributions of fractured samples vary depending on whether samples have been slowly compressed or shocked[19]. Arlery et al.[12] presented data on sand with 10% clay (kaolinite) added in an attempt to "stabilize and homogenize" the water content in their samples. The resulting Hugoniots appear to differ from other literature data on sand, which may be a direct result of the added clay fraction. Other studies suggest that both particle size[20] and material composition[21] affect shock response. In a previous paper[14], we proposed that a small amount of moisture reduces the stress concentration and shear strength at contact points, slowing shock velocity; while in fully saturated samples shock velocity depends on the connectivity of the inter-granular structure.

In this letter, we report a series of experiments on three similar silica sands, highlighting the effects of varying morphology, rate and moisture on compaction. Plate impact experiments have been supplemented by uniaxial, quasi-static (QS) compaction tests with rigid lateral confinement, and post-compaction analysis of grains to determine the extent of fracture.

To compare with the fine "rough" builders' sand used previously[13, 14], we introduce both a "smooth" sand and a "sandy loam" as shown in Figure 1. The smooth sand, Leighton Buzzard "Fraction D" (sourced from David Ball Group, UK), has translucent white grains and a more weathered grain surface, providing a useful intermediary between the majority of sands and widely studied systems of silica spheres. The smooth material also has a slightly larger modal grain size and narrower distribution. The sandy loam is very similar to the rough sand except for the presence of silt (c.10%) and a small organic component (c.1-2%). The rough sand, sandy loam and smooth sand have a very similar mean aspect ratio (0.743, 0.746 and 0.744 respectively), HS circularity (4π.grain area/grain perimeter^2) (0.819, 0.812, 0.812) and convexity (convex hull perimeter / grain perimeter) (0.976, 0.973, 0.975), as determined using a Malvern Morphologi G3. Particle size distributions (PSDs) are given alongside those for recovered samples in Figure 4. The smooth sand is 99.8% quartz, while the rough sand contains 6-7% orthoclase, and the sandy loam 2-3% orthoclase and 1.6-2% goethite. These small impurity fractions were deemed unlikely to significantly affect compaction response. All materials were sieved at 850 μm to remove a small number of large grains, then dried for 24 h at 120 °C to remove residual moisture.

This manuscript was accepted by Appl. Phys. Lett. Click here to see the version of record.

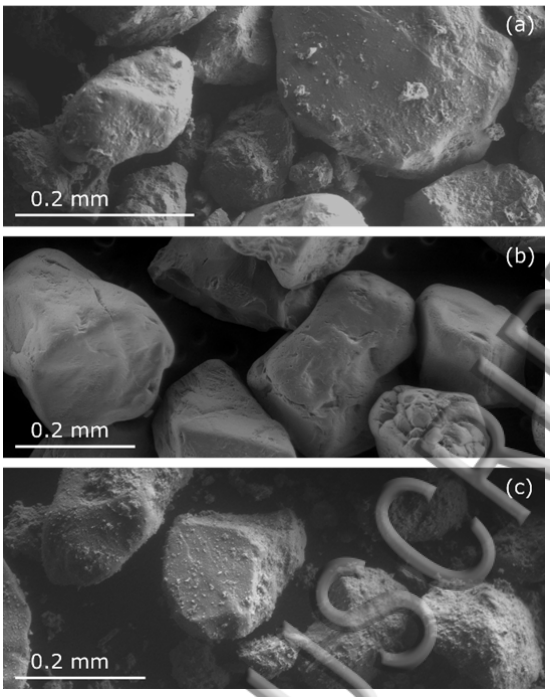

Figure 1: ESEM and optical images of the three sands used: (a) rough sand, (b) smooth sand and (c) sandy loam. While the grains are similarly shaped, the grain surfaces on the smooth sand are substantially more weathered, and the sandy loam contains a number of smaller particles.

Quasi-static compaction experiments were performed on the three dry samples, providing comparative information in order to decouple rate effects from morphological differences, using a method similar to Neal et al[19]. Sand samples were loosely poured into position between 10 mm diameter high strength steel punches and radially confined by a maraging-steel annulus, with an intermediate thin Teflon film to reduce friction. Each sample was loaded to approximately 1.5 GPa at 0.02 mm s^{-1} using an Instron 600KPX universal testing machine. Total axial, radial and frictional (through the lateral walls) forces were recorded. Subtracting the frictional stress from the measured total stress provides the resultant stress through the sand sample, while the recorded punch positions give sample density.

Results (Figure 2) indicate little difference between rough sand and sandy loam, suggesting that at low rate the presence of some silt does not significantly affect compaction. The smooth sand compacts substantially less readily, to the point that by 1.5 GPa, the remaining void fraction (comparing with the compaction curve for z-cut quartz) is roughly 50% greater than that of the other two materials, as shown in Figure 2a. In the smooth sand, an initially stiffer region at low stress indicates yielding of the soil skeleton[5] at approximately 20 MPa, whereas the other two materials do not show any such initial elastic response (Figure 2b).

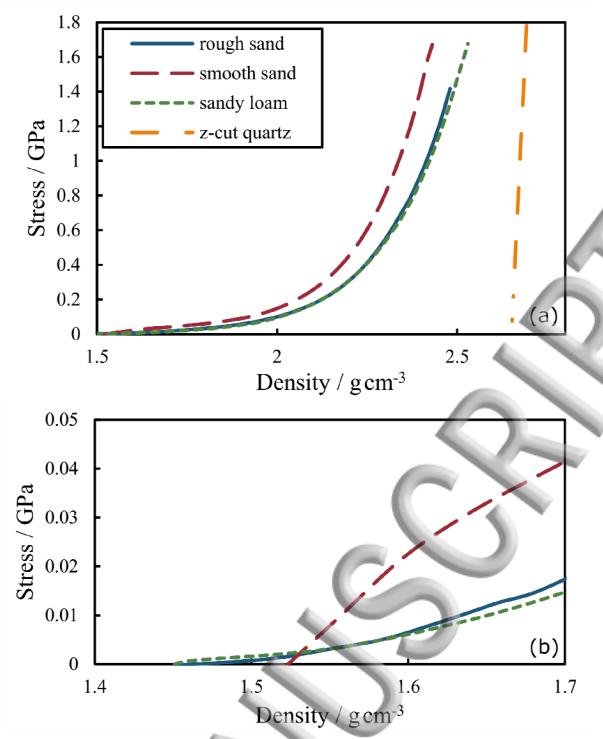

Figure 2: Quasi-static compaction data for the two materials in a gauged reactive (GREAC) cell[22] (a), including a detail of the low-stress region (b).

Plate impact experiments were performed following the method published previously[13, 14]. Smooth sand was tested dry and moist, along with dry sandy loam, and compared to existing dry and moist rough sand results[14]. The addition of any moisture makes the sandy loam highly inhomogeneous on a length scale of several millimetres due to movement and agglomeration of the silt fraction. It was therefore impractical to test moist sandy loam in our 4 mm deep sand cells.

After insertion into a cell, each material was prepared to a "lightly tapped" density, thus ensuring that fracture or structural anisotropy was not induced in the samples due to pre-compaction. This gave densities of rough sand (1.38-1.45) g cm^{-3}, smooth sand (1.58-1.61) g cm^{-3}, and sandy loam (1.43-1.49) g cm^{-3}. 10% moist sand samples were fabricated by mixing dry sand and water in a multi-axial powder mixer, then lightly manually compacting the cells to (1.60-1.64) g cm^{-3} for both materials.

Time-of-flight and impedance matching techniques were employed to give shock velocity, particle velocity and stress in the sand bed, using literature values for the Hugoniots of copper and PMMA[23]. Figure 3 compares the subsequent Hugoniot points in shock-velocity (U_s) *versus* particle-velocity (u_p) space, along with least squares linear fits. Compared with dry rough sand[13], the smooth sand has a flatter Hugoniot, with the lower U_s for a given u_p indicating a lower stiffness than rough sand at higher impact stresses. Even lower shock speeds and increased scatter are observed in the sandy loam, the latter attributed to greater inhomogeneity due to the silt fraction.. Comparing moist smooth sand with moist rough sand[14], we see no discernible difference: the two Hugoniots overlap almost perfectly. All five data sets are confirmed as normally distributed about their linear fits (Shapiro-Wilk[24]). Analysis of covariance[25], based on estimated common gradients to obtain an adjusted mean, gives the differences in shock velocity as (379±47) m s^{-1}

between dry rough sand and sandy loam; (181±50) m s^{-1} between dry rough sand and dry smooth sand; and (37±59) m s^{-1} between the two moist materials.

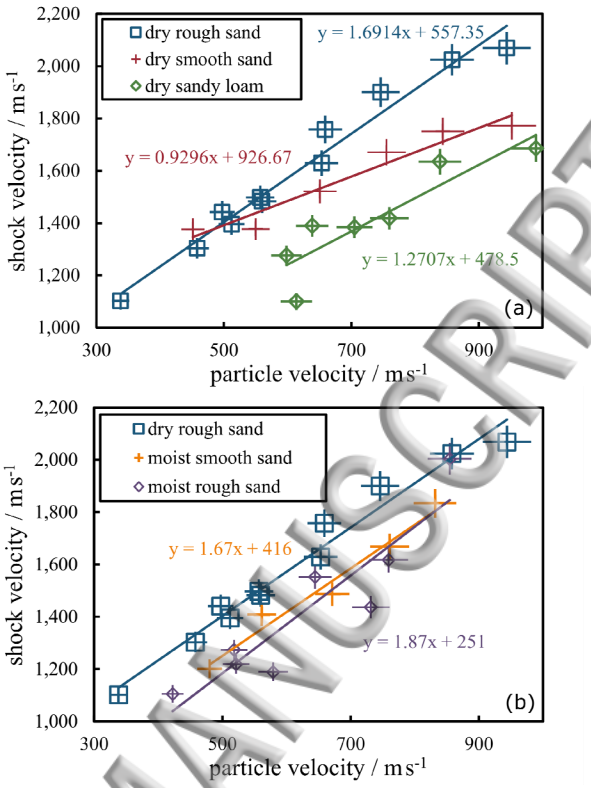

Figure 3: Hugoniot data for (a) the three dry sands and (b) the two moist sands (with dry rough for reference). The Hugoniots of the three dry materials differ substantially, while adding 10% moisture results in both rough and smooth sand behaving similarly. Dry and moist rough sand data reproduced from Appl. Phys. Lett. 107, 174102 (2015), Copyright 2015 AIP Publishing LLC.

To recover shocked sand samples, five capture cells were built and impacted with 50 mm diameter copper flyer plates at 500 m s^{-1}. A 15 mm steel cup held a 3 mm deep, 40 mm diameter sand bed on top of 9 mm of polyethylene glycol 1,000. A 3 mm deep oxygen-free copper front plate ensured that the sample was contained after impact, and this inner cell was housed within a larger aluminium surround. Capture experiments on granular materials pose a particularly challenging set of issues[26], in that the sample will invariably be loaded multiple times. Characterizing the loading history is difficult with stress gauges, which are unreliable for repeated multi-dimensional loading. Simulations using the GRIM Eulerian hydrocode with a compaction EoS (based on experimental QS and plate impact data) and Johnson-Holmquist constitutive model were used to show that the sample 'rings up' to a peak stress of 2-3 GPa, depending on initial density and position within the bed – conditions broadly comparable with the quasi-static data. As the dry and moist materials exhibit similar shock impedances, differences in stress history between experiments will be small. In the case of saturated sand, peak loading stress will be higher, potentially resulting in more grain fracture – however even at this stress, results show fracture is minimal. A Malvern Mastersizer 2000 laser-particle-sizer was used to measure recovered particle size, specifically sphere equivalent radii.

Figure 4 compares the PSD results for the rough sand (4a), smooth sand (4b) and sandy loam (4c); there are clear qualitative differences with moisture and rate. In all cases, the solid blue line shows the PSD of the source material. The corresponding PSD of the shock compacted dry materials is shown by the dotted green lines. In all cases there is a single peak at ~50 μm, with minimal variation between the three sands except for a slightly greater extent of fracture in the smooth sand. Adding moisture has a very significant effect (dashed orange and long-dashed purple lines for rough sand). A single peak in the PSD is still evident, but the shift in modal grain size due to shock-loading is less for wetter samples.

In comparison, the QS compacted (dry) material shows very different behavior. In all cases, the resulting PSD (short-dashed red line) is bimodal, having one peak close to that of the original material, and a second peak close to the position of the peak observed during shock compaction. The three materials behave similarly, although for the smooth sand the peaks are less well separated, resulting in an overall flatter distribution, and with fewer very small grains.

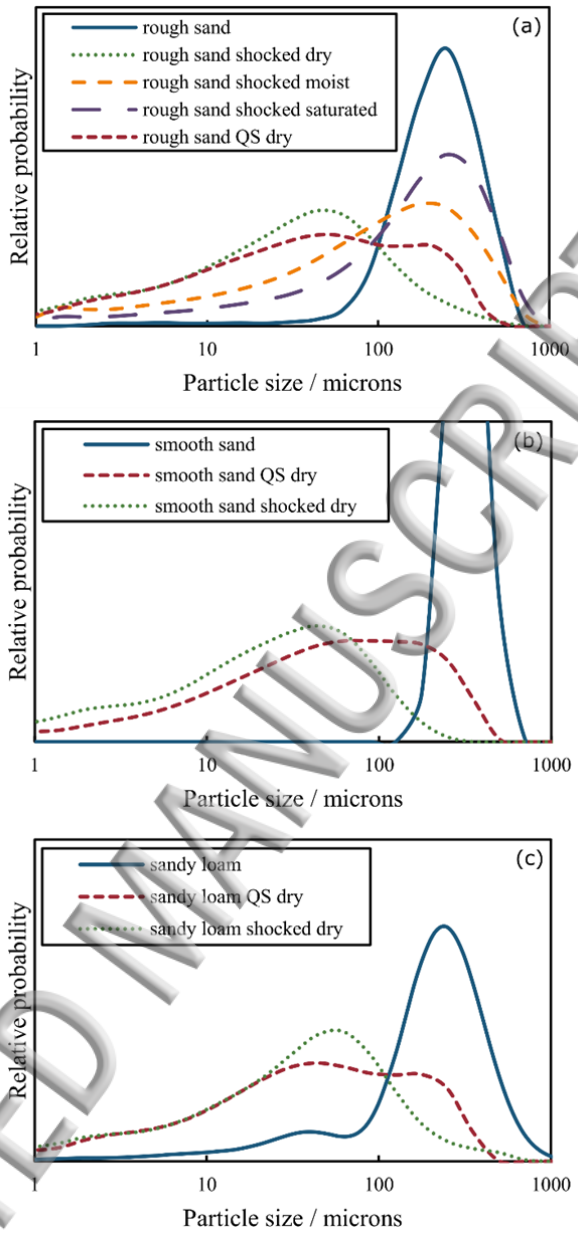

Figure 4: Particle size distributions for initial and compacted materials. Under shock loading, all three materials fracture to a similar extent; under QS loading conditions, the rough sand (a) fractures more readily than the smooth (b), while the rough sand (a) and sandy loam (c) exhibit bi-modal particle size distributions. Moist and saturated shocked samples exhibit substantially less particle fracture (a). Note that all y-axes are scaled equally for ease of comparison.

These apparently complex differences in behaviour, seen as a result of varying rate, morphology and moisture, can all be explained by considering grain-scale processes. Fracture and rearrangement are interlinked processes ongoing throughout compaction, with at least a small amount of fracture generally required to facilitate substantial rearrangement. During compaction, even very small applied stresses overcome frictional forces and begin to fracture weak structures in the rough sand (primarily abrasion and attrition), resulting in the comparatively soft response with an apparent yield stress of zero. Conversely, the stiffer initial compaction region in the smooth sand (Figure 2b) is indicative of a lack of fracture below approximately 20 MPa[5].

At higher stresses, the smooth sand is more able to re-configure itself (in response to ongoing fracture as loading stress is increased) such that force chains carrying stress through the material are relatively evenly distributed, engaging a high percentage of the bulk in resisting compaction, leading to the steeper curve in Figure 2a. In the rough sand the stress distribution is less even, so some contact points – jammed in place by inter-granular friction – experience very high stresses, leading initially to more uneven fracturing of grains. The preferential fracture of certain grains naturally leads to the bimodal PSD, a process more evident in the rougher sand. Bimodality may be further enhanced through feedback whereby fines effectively "cushion" the remaining larger grains by increasing co-ordination number[27], counteracting the usual preferential fracturing of larger grains[28]. These fines are present initially in the sandy loam, and created at low stresses by attrition in the rough sand; the effect is less prevalent in the smooth sand, where the post-compaction fines content is lower.

Under shock loading the processes are quite different; the main observations being different compaction behaviour between all three dry sands, and a unimodal PSD. During shock there is insufficient time for substantial grain re-arrangement, and the supersonic nature negates significant stress propagation ahead of the compaction front – so the concept of force chains or a granular backbone is largely inapplicable. Instead, the shock-compaction wave progresses through the material, affecting all the grains and resulting in the unimodal PSDs observed. In support of this hypothesis, consider that grain fracture probability due to loading a single grain generally follows a log-normal distribution[29]. As a function of particle number (not shown) the PSDs of all the shocked samples closely follow log-normal distributions, consistent with the stress state under shock loading not being controlled by complex (multi-grain) force chain interactions.

The differences seen at the shock front are based on the nature of inter-grain contact points. We have seen previously[14] that the addition of a little moisture slows the shockwave, while full saturation results in two different shock Hugoniots depending on inter-grain connectivity. Similarly, the fine particles in the sandy loam appear to soften the contact points between larger grains, reducing the peak stresses and resulting in its very low shock impedance (Figure 3a). The fines that soften the interaction in the rough sand during quasi-static loading are created during the loading process, hence the divergent behavior of the two materials under shock conditions.

Under shock loading the dry smooth sand is softer than the rough at higher stresses, in contrast with the results for quasi-static compaction, but the mechanisms for this remain unclear. The lower shock speed may be a result of reduced stress-focusing in the smooth sand, arising in part from a higher mean co-ordination number in the initially denser smooth sand samples. Furthermore, one recent model[17] predicts that an increase in friction will accelerate grain locking and increase the inelastic response, resulting in a higher wave speed and reduced dispersion. The addition of moisture has a consistent effect on shock response: although materials respond quite differently when dry (Figure 3a), both the rough and smooth sands behave almost identically when moist (Figure 3b), in agreement with the trend predicted by Borg *et al*[30]. Here, the grain-grain contacts become defined by localized moisture rather than surface texture. Given that the Hugoniot for moist rough sand is much closer to that for dry than saturated[14], the minimal fracture observed for moist sand strongly suggests shock speed is not controlled by the extent of grain fracture.

Overall, we have studied three silica sands with similar modal grain sizes and initial bulk densities. We have established fundamental qualitative differences in the granular response to loading at different rates:

- At **low rate**, grain morphology and surface texture is dominant; smoother grains are more readily able to re-configure and "spread the load", while in rougher sands inter-granular friction inhibits the process. Preferential fracture of certain highly loaded or weak grains leads to a bimodal particle size distribution, with fines (present initially or produced through abrasion and attrition of rough asperities) enhancing the process.
- At **high rates**, grain rearrangement is suppressed, so morphological differences have less effect. Instead, the compaction wave is dominated by contact point shock-coupling, which can be modified by moisture or fines. Grain surface roughness also affects shock response, though the origin of this phenomena is not yet fully understood. Shock loading affects all grains without the multi-grain interactions of extensive force chains, leading to a unimodal distribution of fractured grain sizes.

We have demonstrated that microscopic properties are strongly coupled with the macroscopic compaction response of brittle granular materials, and provided a set of experimental procedures for probing these phenomena. Crucially, this insight regarding which grain-scale phenomena are relevant in each regime provides a valuable aid for developing accurate morphology- and rate-sensitive material models, both continuum and discrete. More generally, our insights help establish a roadmap towards a more comprehensive description of granular compaction, and the long term goal of developing "designer" granular materials with dynamic properties to suit specific requirements.

Acknowledgements: This research was supported through the FPE research programme led by QinetiQ plc. on behalf of DSTL, with additional support from the Avik Chakravarty Memorial Fund. We thank C. J. Rolfe for technical assistance and P. Gould and P. Church of QinetiQ for their interest and modelling support.

References

1. E. Buhl, M. H. Poelchau, G. Dresen and T. Kenkmann, Meteoritics and Planetary Science **48**, 71-86 (2013).

2. A. Collins, J. Addiss and W. Proud, AIP Conference Proceedings **1195**, 1443-1446 (2009).

3. M. N. Toksöz, C. H. Cheng and A. Timur, Geophysics **41**, 621-645 (1976).

4. R. Blumenfeld, S. F. Edwards and S. M. Walley, in *The Oxford handbook of soft condensed matter*, edited by E. M. Terentjev and D. A. Weitz (Oxford University Press, Oxford, 2015), pp. 167 - 231.

5. M. Omidvar, M. Iskander and S. Bless, Int J Impact Eng **49**, 192-213 (2012).

6. K. Tsembelis, W. G. Proud, B. A. M. Vaughan and J. E. Field, in *Behaviour of Materials at High Strain Rates: Numerical Modelling*, edited by F. G. Benitez (DYMAT, Saint-Louis, France, 2002), pp. 193 - 203.

7. D. J. Chapman, K. Tsembelis and W. G. Proud, AIP Conference Proceedings **845**, 1445-1448 (2005).

8. J. L. Brown, T. J. Vogler, D. E. Grady, W. D. Reinhart, L. C. Chhabildas and T. F. Thornhill, AIP Conference Proceedings **955**, 1363-1366 (2007).

9. D. J. Chapman, C. H. Braithwaite and W. G. Proud, AIP Conference Proceedings **955**, 1367-1370 (2007).

10. M. D. Dianov, N. A. Zlatin, S. M. Mochalov, G. S. Pugachev and L. K. Rosomakho, Soviet Technical Physical Letters **2**, 207-208 (1976).

11. D. J. Chapman, K. Tsembelis and W. G. Proud, in *Annual Conference and Exposition on Experimental and Applied Mechanics* (Society for Experimental Mechanics, Bethel CT, 2006).

12. M. Arlery, M. Gardou, J. M. Fleureau and C. Mariotti, Int J Impact Eng **37**, 1-10 (2010).

13. C. H. Braithwaite, J. I. Perry, N. E. Taylor and A. P. Jardine, Appl Phys Lett **103**, 154103 (2013).

14. J. I. Perry, C. H. Braithwaite, N. E. Taylor and A. P. Jardine, Appl Phys Lett **107**, 174102 (2015).

15. X. Zheng and D. Wang, Acta Mechanica Solida Sinica **23**, 579 (2010).

16. E. S. Hertel, R. L. Bell, M. G. Elrick, A. V. Farnsworth, G. I. Kerley, J. M. Mcglaun, S. V. Petney, S. A. Silling, P. A. Taylor and L. Yarrington, in *Shock waves @ Marseille I* (Springer, 1995), pp. 377-382.

17. S. K. Dwivedi, L. Pei and R. Teeter, J Appl Phys **117** (8), 085902 (2015).

18. W. D. Neal, D. J. Chapman and W. G. Proud, AIP Conference Proceedings **1426**, 1443-1446 (2011).

19. W. D. Neal, G. J. Appleby-Thomas and G. S. Collins, Journal of Physics: Conference Series **500**, 112047 (2014).

20. A. M. Bragov and G. M. Grushevskii, Tech Phys Lett+ **19**, 385-386 (1993).

21. E. Suescun-Florez, S. Kashuk, M. Iskander and S. Bless, Journal of Dynamic Behavior of Materials **1** (3), 330-346 (2015).

22. A. J. Sheridan and A. D. Pullen, Magazine of Concrete Research **66** (1), 50-59 (2014).

23. S. P. Marsh, *LASL Shock Hugoniot data*. (University of California Press, Los Angeles, CA, 1980).

24. S. S. Shapiro and M. B. Wilk, Biometrika **52**, 591-611 (1965).

25. D. C. Montgomery, *Design and Analysis of Experiments*, 8th ed. (John Wiley & Sons, 2012).

26. B. J. Marr, O. E. Petel, D. L. Frost, A. J. Higgins and S. Ringuette, Journal of Physics: Conference Series **500**, 112044 (2014).

27. J. Huang, S. Xu and S. Hu, Int J Impact Eng **59** (0), 1-10 (2013).

28. F. A. Chuhan, A. Kjeldstad, K. Bjørlykke and K. Høeg, Mar Petrol Geol **19** (1), 39-53 (2002).

29. S. Aman, J. Tomas and H. Kalman, Chemical Engineering Science **65** (5), 1503-1512 (2010).

30. J. P. Borg and T. J. Vogler, presented at the International Conference on the Mechanical and Physical Behaviour of Materials under Dynamic Loading (DYMAT), Les Ulis, France, 2009 (unpublished).

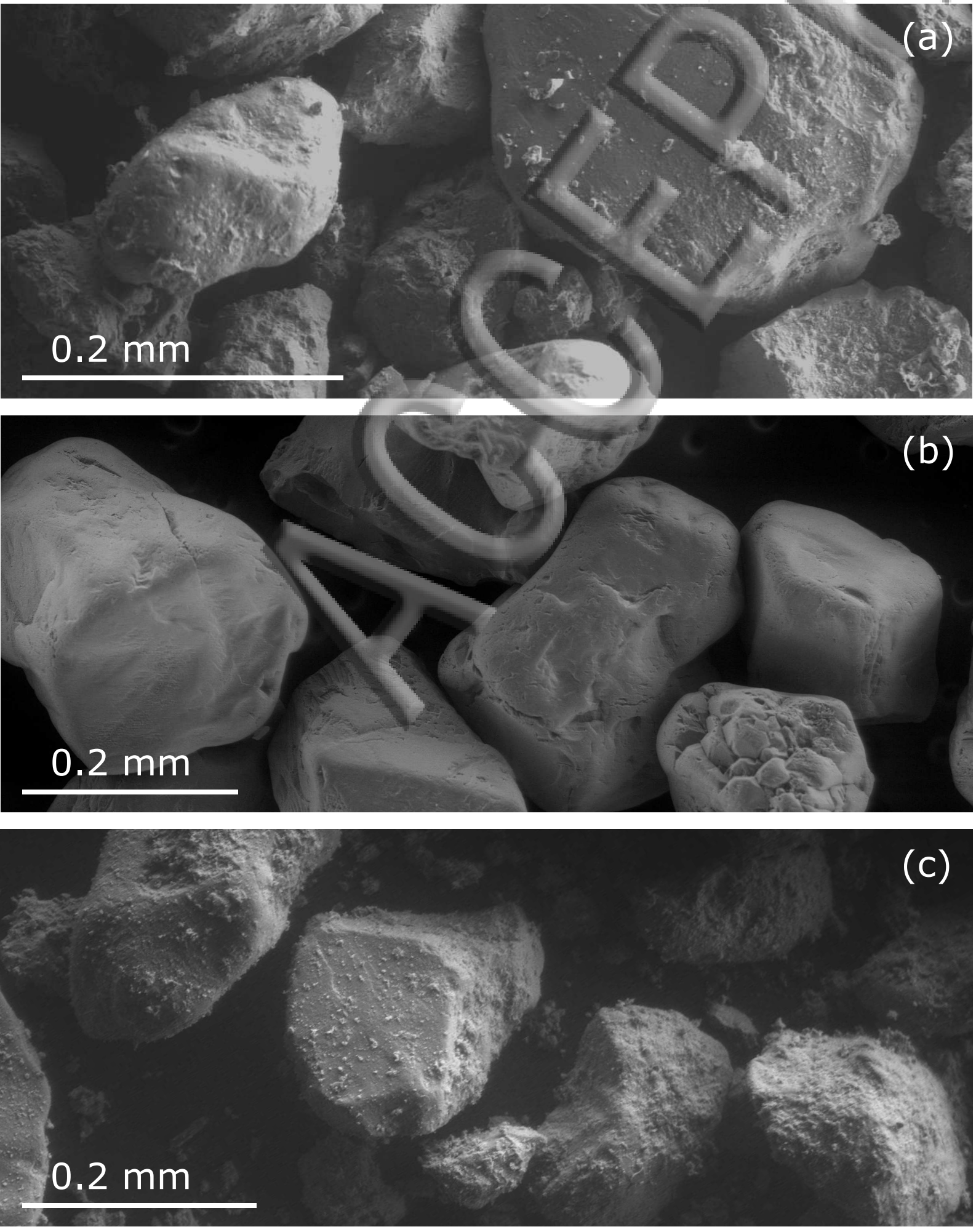
(a)
0.2 mm
(b)
0.2 mm
(c)
0.2 mm

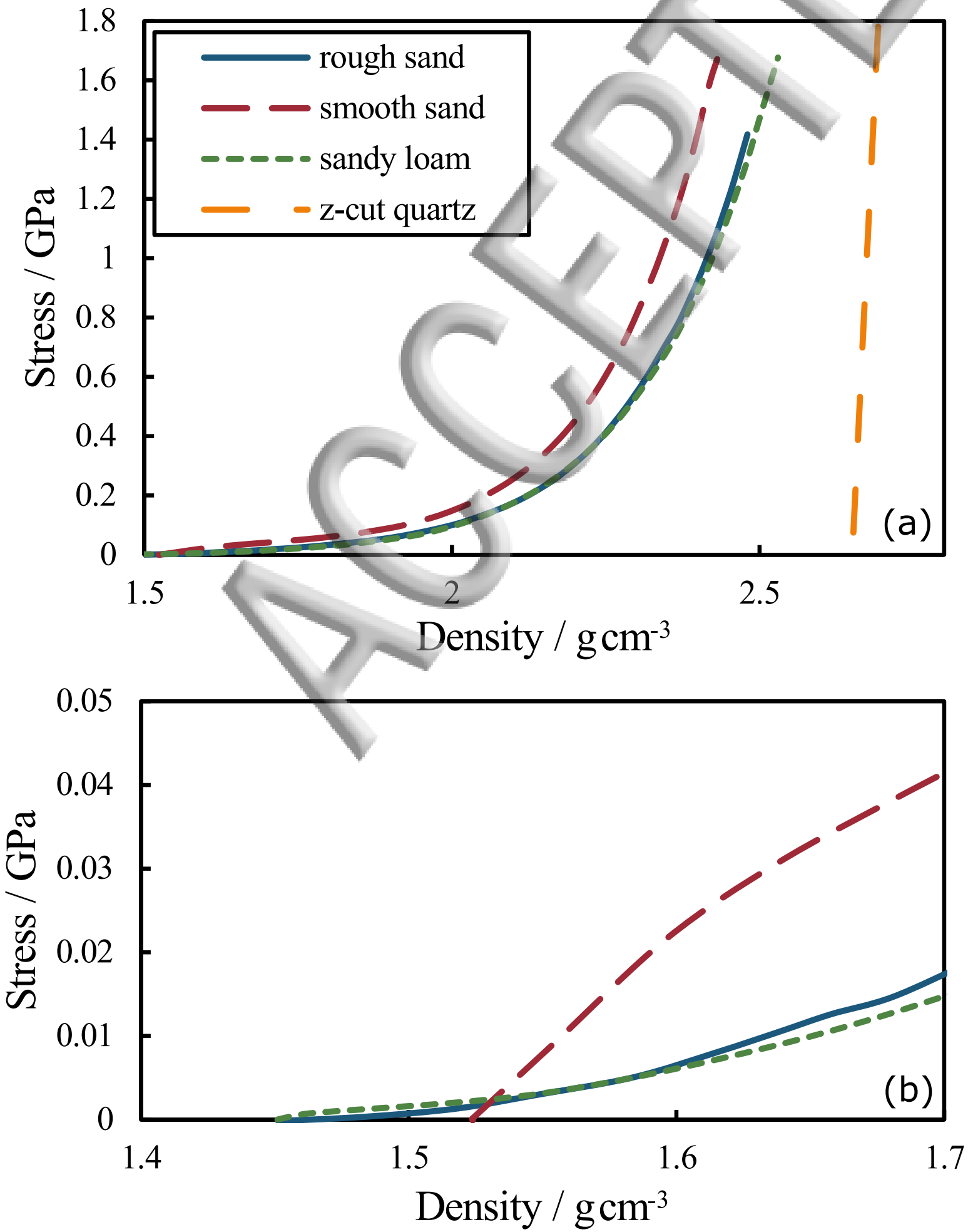
rough sand
smooth sand
sandy loam
z-cut quartz
Stress / GPa
Density / g cm-3
(a)
(b)

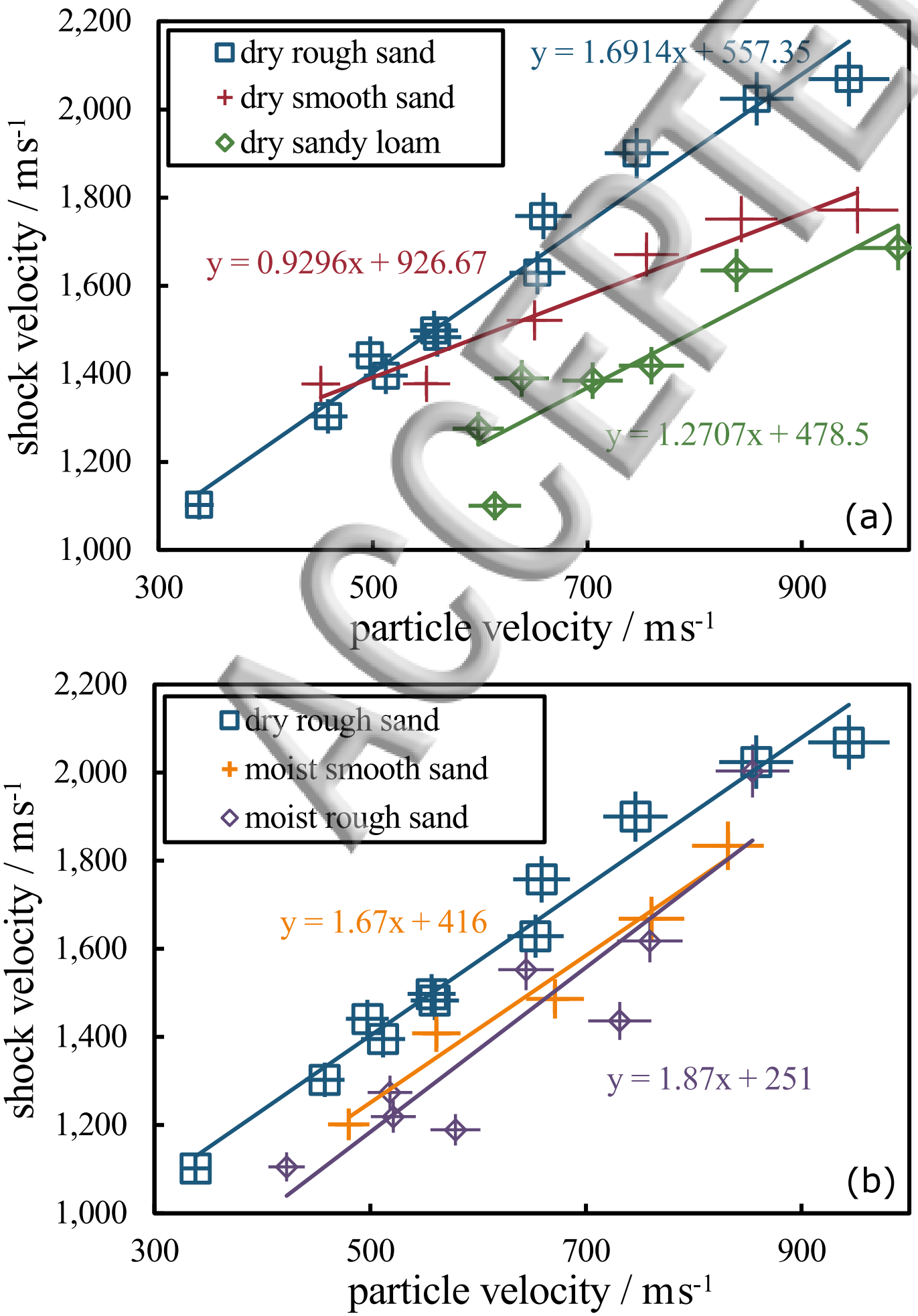
dry rough sand
dry smooth sand
dry sandy loam
y = 1.6914x + 557.35
y = 0.9296x + 926.67
y = 1.2707x + 478.5
(a)
shock velocity / ms-1
particle velocity / ms-1
2,200
2,000
1,800
1,600
1,400
1,200
1,000
300
500
700
900
dry rough sand
moist smooth sand
moist rough sand
y = 1.67x + 416
y = 1.87x + 251
(b)
shock velocity / ms-1
particle velocity / ms-1

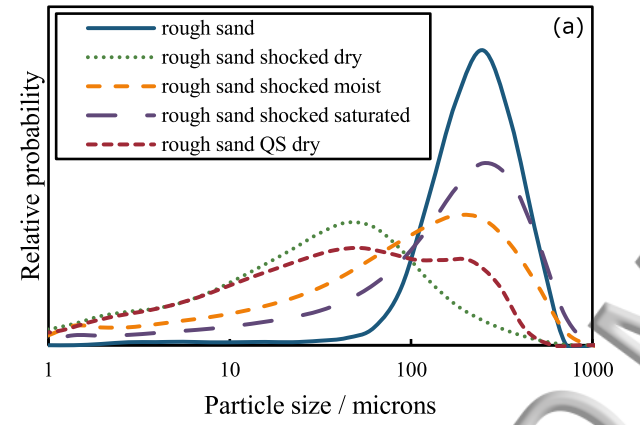
rough sand
rough sand shocked dry
rough sand shocked moist
rough sand shocked saturated
rough sand QS dry
(a)
Relative probability
1
10
100
1000
Particle size / microns

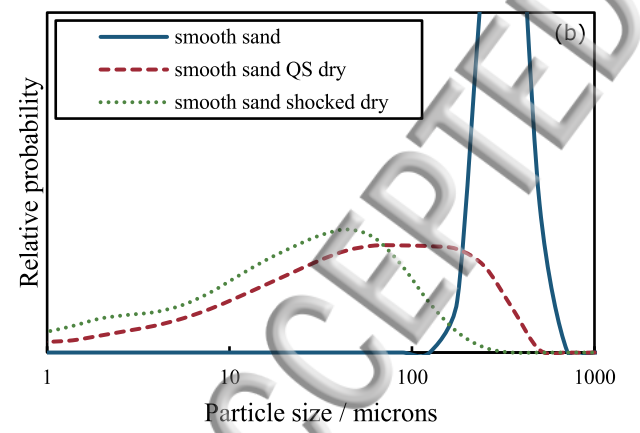
smooth sand
smooth sand QS dry
smooth sand shocked dry
(b)
Relative probability
1
10
100
1000
Particle size / microns

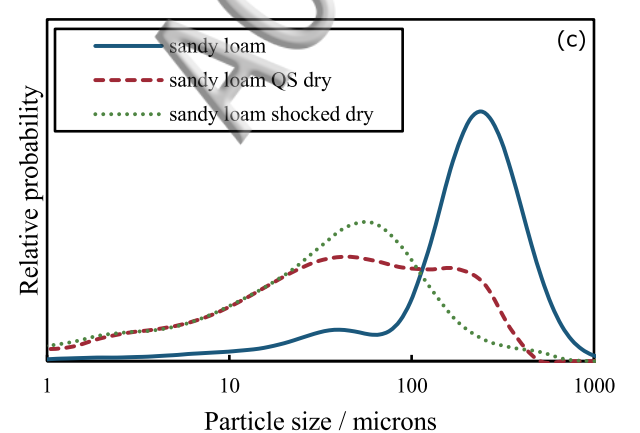
sandy loam
sandy loam QS dry
sandy loam shocked dry
(c)
Relative probability
1
10
100
1000
Particle size / microns